Astron. Astrophys. 343, L83–L86 (1999)

ASTRONOMY AND ASTROPHYSICS

Letter to the Editor

The H_2O abundance and star formation history in ρ Oph*

René Liseau and Göran Olofsson

Stockholm Observatory, S-133 36, Saltsjöbaden, Sweden (rene; olofsson@astro.su.se)

Received 15 December 1998 / Accepted 14 February 1999

Abstract. ISO-LWS observations towards a large number of different positions in the core of the ρ Oph cloud are used to place a limit to the abundance of wide spread H_2O. From NLTE excitation and radiative transfer modelling the average line spectrum of the ρ Oph cloud, we find $X(H_2O) < 10^{-6}$ to 10^{-5}. We interprete these results within the framework of the dynamical chemistry models by Bergin, Melnick & Neufeld (1998), which describe the time evolution of molecular clouds being shocked by outflowing gas from young stellar objects, and conclude that the ρ Oph cloud has been forming stars for less than one million years ($2 - 5 \times 10^5$ yr). Finally, we show that this limiting result can be put to conclusive observational test by the ODIN satellite mission in the near future.

Key words: ISM: individual objects: ρ Oph cloud (L 1688) – ISM: clouds – ISM: abundances – ISM: molecules – ISM: jets and outflows – stars: formation

1. Introduction

The eastern regions (L 1688) of the active star forming ρ Ophiuchi clouds are confined to an area of $1\,\mathrm{pc} \times 2\,\mathrm{pc}$ at the distance of roughly 150 pc. The surface density of young stellar objects, which have been identified on the basis of their infrared excess (IR), is high, i.e. $N_{\rm IR} \sim 100\,\mathrm{pc}^{-2}$ (Bontemps et al. 1999 and references therein).

During the early phases of their evolution, young stellar objects commonly develop powerful outflows, which affect their surroundings and, perhaps, regulate the matter infall and accretion rates for the forming stars (Lada 1985; Shu et al. 1987). Outflows and shocked gas are known to exist at present in the ρ Oph cloud (Tamura et al. 1990, André et al. 1993, Sekimoto et al. 1997, Wilking et al. 1997, Gómez et al. 1998). After a typical flow time of $\tau_{\rm f} \sim 2 \times 10^4$ yr (Staude & Elsässer 1993), these outflows have reached average distances $0.2\,(v_{\rm f}/10\,\mathrm{km\,s^{-1}})\,(\tau_{\rm f}/2 \times 10^4\,\mathrm{yr})$ pc, so that they have filled (at least partially) a volume $0.2^3 \sim 10^{-2}\,\mathrm{pc}^3$.

Based on the column density map of ρ Oph by Wilking & Lada (1983) and the average density $n(H_2) = 2 \times 10^4\,\mathrm{cm}^{-3}$ determined by Liseau et al. (1995, 1999), the depth of the cloud along the line of sight is of the order of 1 pc. The *volume* density of IR-objects is numerically comparable, therefore, to $N_{\rm IR}$. This suggests that the available space is filled with outflow gas ($v_{\rm f} \geq 10\,\mathrm{km\,s^{-1}}$) by the time of $\lesssim 10^5$ yr. If star formation is not strictly coeval, as is suggested by the coexistence of Class 0 and Class I–III sources in ρ Oph, the timescale of space filling by the outflows would be longer by one to two orders of magnitude, i.e. 10^6–10^7 yr.

For timescales of this order, Bergin et al. (1998, hereafter BMN) have calculated dynamical models of the shock chemistry in molecular clouds, which become pervaded by generations of outflows from young stellar objects. These models predict the time averaged abundance of gas phase water, $X(H_2O)$, as a function of the cloud evolution timescale.

In this *Letter*, we are persuing the proposal by BMN that the abundance of H_2O can be used to follow the shock history, and hence also the star formation history, of the molecular cloud. We base the discussion on the results of ISO-LWS[1] observations, which are briefly described in Sect. 2. In Sect. 3, we introduce NLTE excitation and radiative transfer models of H_2O emission and apply the results to estimates of the abundance of wide spread H_2O in the ρ Oph cloud. These results are discussed in the light of the models by BMN in Sect. 4 and in Sect. 5, we summarise the conclusions from this work.

2. Observations and results

The details regarding the observations discussed below have been presented by Liseau et al. (1999). Full spectral LWS scans (43–197 μm) have been obtained towards 33 positions spread over the ρ Oph cloud. The spectral resolution corresponds to more than 1 000 $\mathrm{km\,s^{-1}}$, so that lines from galactic dark clouds are not resolved. The beam size of the LWS is $\sim 1\farcm3$. In Fig. 1, we present the grand average line spectrum between 140 and

Send offprint requests to: R. Liseau

* Based on observations with ISO, an ESA project with instruments funded by ESA Member States (especially the PI countries: France, Germany, the Netherlands and the United Kingdom) and with the participation of ISAS and NASA.

[1] Infrared Space Observatory: Kessler et al. (1996); Long Wavelength Spectrometer: Clegg et al. (1996), Swinyard et al. (1996).

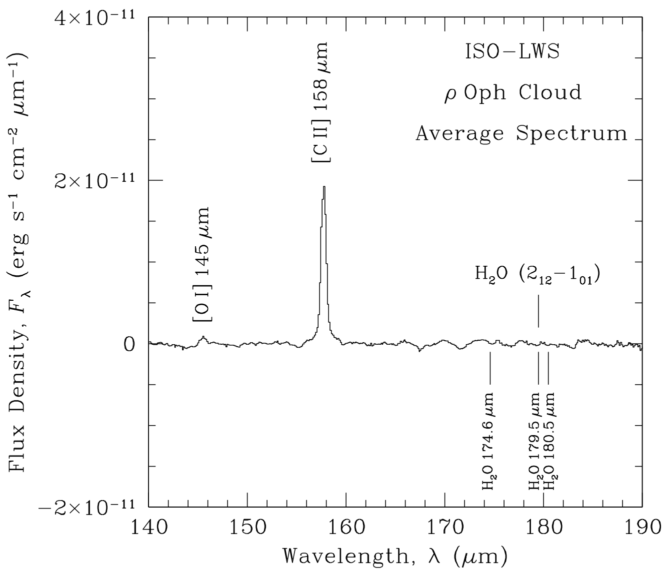

Fig. 1. The average line spectrum (continuum subtracted) between 140 and 190 μm for 33 positions spread over the ρ Oph cloud. The emission lines [O I] 145 μm ($^3P_0$ - $^3P_1$) and [C II] 158 μm ($^2P_{3/2}$ - $^2P_{1/2}$) are clearly seen. Below the spectrum, the wavelengths of three ortho-H_2O lines, discussed in the text, are indicated

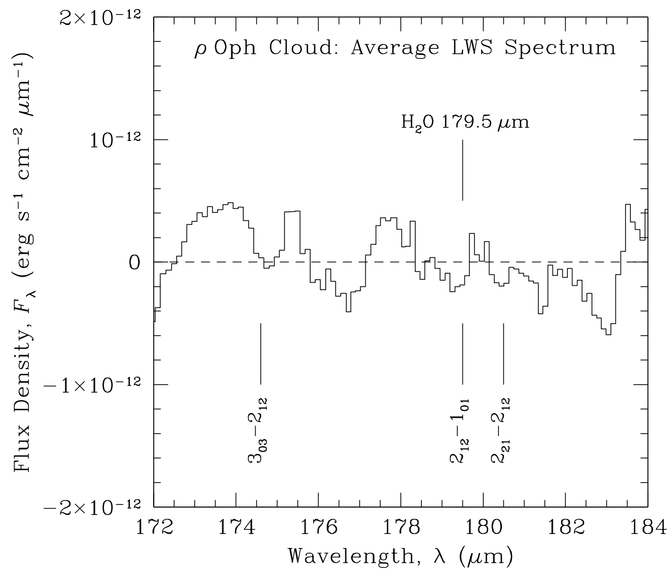

Fig. 2. Enlargement of the spectrum shown in Fig. 1. The positions of the rotational transitions of the H_2O lines, discussed in the text, are indentified and labelled with their respective quantum numbers. The resolution of the long wave spectrum of the LWS is 0.6 μm (FWHM). Broad features are residuals from insufficient de-fringing

190 μm, obtained from 261 individual spectral scans for a total time of integration of 12.7 hr. A blow-up of this figure, at expanded scale, is shown in Fig. 2. Prior to averaging, spectral fits to the continuum had been subtracted, so that the rms-noise fluctuates about the zero-level. Extended emission gives rise to fringes in LWS observations and the wavy appearance in the figures is due to residuals from the non-perfect de-fringing of the individual spectra. In the interval 160 to 190 μm, the value of the rms-noise has been determined as 2.5×10^{-13} erg cm^{-2} s^{-1} μm^{-1} (2.7 Jy).

In Fig. 1, the average line emission from the ρ Oph cloud in [O I] 145 μm ($^3P_0$ - $^3P_1$) and in [C II] 158 μm ($^2P_{3/2}$ - $^2P_{1/2}$) is clearly discernable, whereas molecular lines are not detected. The H_2O line in the wavelength range of the LWS, which could be expected to be the strongest, is the $(2_{12} - 1_{01})$ line at 179.5 μm, connecting to the ground state of ortho-H_2O. For the spectral resolution of 0.6 μm, we place an upper limit to the flux of F(179.5 μm) $< 1.5 \times 10^{-13}$ erg cm^{-2} s^{-1} (1σ). This limit applies also for the other transitions, having upper energies $E/k < 200$ K and their lower level in common with the upper one of the 179.5 μm line, viz. $(3_{03} - 2_{12})$ 174.6 μm and $(2_{21} - 2_{12})$ 180.5 μm (see: Fig. 2).

3. The H_2O abundance in the ρ Oph cloud

In order to estimate the amount of wide spread water vapour which at most can be present in the ρ Oph cloud, we have performed NLTE excitation and radiative transfer calculations for water using a multi-level LVG-code (Large Velocity Gradient), with Einstein transition probabilities from Chandra et al. (1984). Rate coefficients for collisions with H_2 were adopted from Phillips et al. (1996). Detailed balance arguments cannot be used and complete rates for para-H_2 (J = 0, 2) and ortho-H_2 (J = 1) can be obtained for the five lowest levels of ortho-H_2O, which however is sufficient for the average physical conditions encountered in the ρ Oph cloud. The ortho-to-para ratio introduces some uncertainty and we used thermally weighted rate coefficients for 'hybrid-H_2'. For H_2O, presumably formed behind shocks, an ortho-to-para ratio of three-to-one was assumed throughout.

Molecular line observations of the ρ Oph cloud reveal line profiles about 3 km s^{-1} wide at half maximum, with individual components having a FWHM $\sim$ 1.5 km s^{-1}. For most models, both the line width (3 km s^{-1}, i.e. $dV/dr = 3$ km s^{-1} pc^{-1}), the average density on scales 1′ to 2′ ($n(H_2) = 2 \times 10^4$ cm^{-3}), and the dust parameters ($T_{\rm dust} = 30$ K, $\tau_{60\,\mu m} = 5 \times 10^{-2}$, emissivity index = 1.5) were held fixed. Grids of models, for different gas kinetic temperatures, were then computed, varying the water abundance, $X(H_2O)=N(H_2O)/N(H_2)$.

The reliability of the LVG code was tested by comparisons with limiting analytical results. For instance, the flux in an emission line (from a two-level system) can be approximated by

$$F = h\,\nu\,\frac{\Omega}{4\,\pi}\,X_{\rm mol}\,N({\rm H_2})\,\gamma_{\rm lu}\,n({\rm H_2})\,\frac{\frac{\beta_{\rm e}\,n_{\rm c}}{n({\rm H_2})}}{\frac{\beta_{\rm e}\,n_{\rm c}}{n({\rm H_2})}+\frac{\gamma_{\rm lu}}{\gamma_{\rm ul}}+1}\,,$$

where the symbols have their usual meaning. Specifically, γ is the collision rate coefficient for the transition(s) $l \leftrightarrows u$, $n_{\rm c} = A_{\rm ul}/\gamma_{\rm ul}$ is the critical density of the transition and $\beta_{\rm e}$, the photon escape probability, is a function of the optical depth in the line (e.g. in slab geometry, $\beta_{\rm e} = (1 - \exp -\tau)/\tau$). As $X_{\rm mol} \to 0$, $\beta_{\rm e}$ tends to unity and the LVG formalism reduces to the ordinary expression for optically thin line emission. In the case of

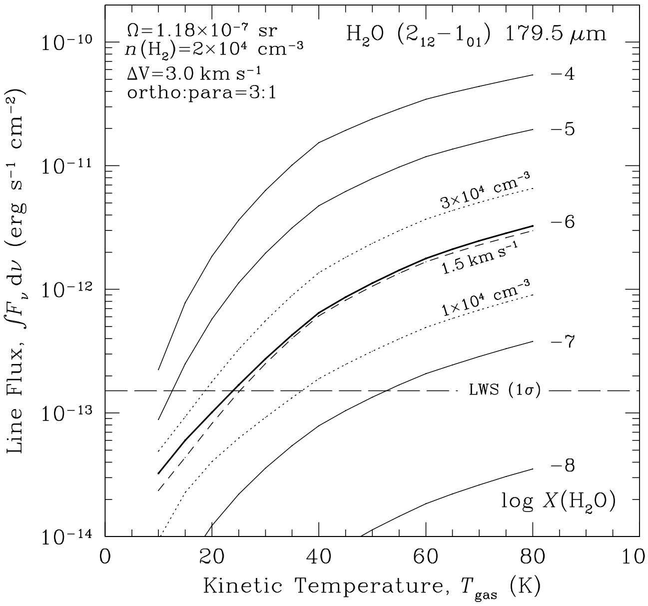

Fig. 3. A grid of NLTE models for the 179.5 μm line of H_2O ($2_{12}-1_{01}$). The line flux is given for a range of gas temperatures, with the water abundance as a parameter and indicated next to each solid curve. The other model parameters are given in the upper left corner. The short-dashed line refers to the model for $X(H_2O) = 10^{-6}$, but for a different line width (1.5 km s^{-1}) and the dotted curves are for two models with different densities. The long-dashed horizontal line refers to the 1σ upper limit to the line flux towards the ρ Oph cloud, obtained from the LWS average spectrum of Fig. 1

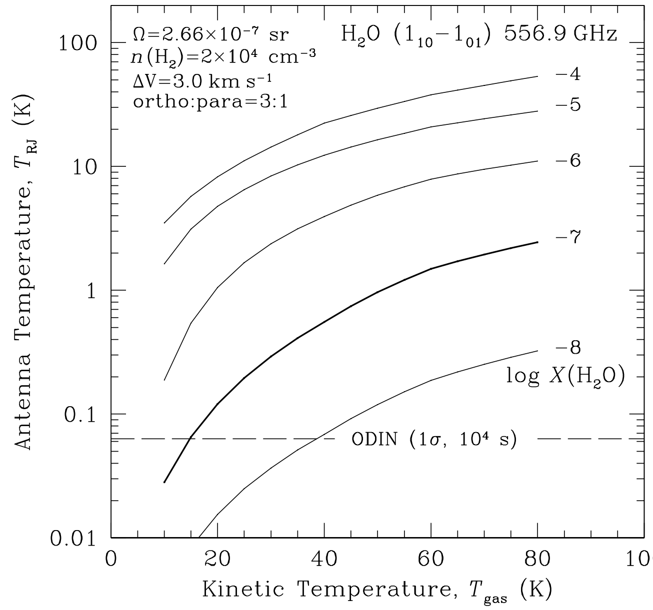

Fig. 4. Same as Fig. 3, but for an observation of the ρ Oph cloud in the 557 GHz ground state line of ortho-H_2O with ODIN (2′ beam). The shown expected 1σ level is reached after 10^4 s, including chopping, and refers to the spectral resolution of 1 MHz (0.5 km s^{-1}). The line strength is in the antenna temperature scale (Rayleigh-Jeans). In order to compare with Fig. 3, the conversion $\int F_\nu d\nu$ (erg cm^{-2} s^{-1}) = 1.4×10^{-13} T_{RJ} (K) can be used (line width 3 km s^{-1})

$X(H_2O) = 10^{-8}$ and subthermal excitation (see below; effectively, the last factor equals unity), the result of the multi-level LVG-program (no dust) is essentially that of the analytical expression above.

The results, relevant to the LWS observations of the 179.5 μm line, are displayed in Fig. 3. In the outmost layers of the cloud, gas temperatures are as high as 60 K, whereas the bulk of the ρ Oph gas is at temperatures significantly lower than this, $T_{gas} \sim 25$ K (Liseau et al. 1999 and references therein). For 25 K and the 'standard model', an upper limit to the water abundance of $X(H_2O) < 10^{-6}$ is indicated by the results in Fig. 3. Narrowing the line width to 1.5 km s^{-1} would have only marginal effects on this result; however, were temperatures or densities much below the assumed values, this limit would be pushed upwards (e.g., towards 10^{-5} for $T_{gas} \sim 10$ K or for $n(H_2) \lesssim 1 \times 10^4$ cm^{-3}, see: Fig. 3). These numbers are merely meant to be illustrative and largely lack relevance for the actual conditions in the ρ Oph cloud: from our ISO-LWS observations we deduce that densities are generally higher than 10^4 cm^{-3}; in addition, very low gas temperatures are encountered only in localised regions, such as in the centre of the dense core ρ Oph B.

4. The star formation history of the ρ Oph cloud

In the models of BMN, a low water abundance is obtained for cold quiescent gas ($X(H_2O) \sim 10^{-7}$, for $T_{gas} < 200$ K at all times), whereas in dynamically active clouds, where parcels of gas go through shocks, values of $X(H_2O) < 10^{-6} - 10^{-5}$ would indicate an outflow activity for times shorter than $10^6 - 2 \times 10^6$ years (see: Figs. 14 & 15 of BMN). Taking the four times higher cosmic ray ionisation rate (see: references in Liseau et al. 1999) into account lowers these limits to the 'shock timescale' (BMN) to approximately $2 - 5 \times 10^5$ years in the ρ Oph cloud.

This could mean either (1) that only relatively few stars in ρ Oph develop powerful outflows during their earliest stages or (2) that the cloud has been forming stars for less than a few times 10^5 to 10^6 years. On the basis of NIR spectroscopy for a number of objects in the ρ Oph cloud, Greene & Meyer (1995) estimated a median age for these stars of about 3×10^5 yr, with an upper limit of 3×10^6 yr. This result has recently been reinforced by Bontemps et al. (1999) who, combining ground-based with ISO observations for a considerably larger number of objects, find $0.2 - 2 \times 10^6$ yr. Comparison with our result strongly supports option (2), i.e. the conclusion that the ρ Oph cloud has formed stars for at most a million years.

It would, nevertheless, be highly desireable to confirm these results by an actual detection. We are confident that this check will be performed in the near future: the dedicated satellites SWAS (Melnick et al. 1997)[2] and ODIN (Nordh 1997) are about to become operational and will be able to observe the cloud in the ($1_{10} - 1_{01}$) ground state line of ortho-H_2O at 556.9 GHz (538.3 μm). Models of the physical conditions

[2] SWAS was successfully launched on December 5, 1998.

prevailing in the ρ Oph cloud generally predict the 557 GHz line to be much stronger than the 179.5 μm line. The heterodyne technique has the further advantage that it permits observations at very high spectral resolution ($\gtrsim 4 \times 10^6$, yielding $\Delta v \sim 0.07$ km s^{-1}). Narrow lines as those expected from the ρ Oph cloud would become resolved and their detailed profiles could be studied. This is particularly warranted as the *proper* determination of the H_2O abundance from these optically very thick lines [$\tau \gtrsim 10^2$ (10^3) for $X(H_2O) = 10^{-7}$ (10^{-6})] would require the knowledge of the line shape (Hartstein & Liseau 1998).

In Fig. 4, calculations similar to those of Fig. 3, but for the 557 GHz line are presented. Using current sensitivity estimates for ODIN, an observation of ~ 3 hr would result in an rms-noise of 0.07 K. This would clearly be pushing the ISO-LWS limit towards either a detection by ODIN or a very sensitive and significant upper limit ($X(H_2O) \sim 10^{-7}$, see above). Given the large number density of Class I sources and outflows, the BMN model is certainly relevant to the evolution of the ρ Oph cloud. We can expect, therefore, that either of the two possible ODIN scenarios should provide very important insight into the star formation history of the ρ Oph cloud.

5. Conclusions

The main conclusions from this work can be summarised as follows:

- ISO-LWS observations of the star forming ρ Ophiuchi cloud resulted merely in upper limits to the flux of lines from wide spread water in the gas phase. In particular, $F(179.5\,\mu\mathrm{m}) < 1.5 \times 10^{-13}$ erg cm^{-2} s^{-1} (1σ).
- Results of H_2O NLTE excitation and radiative transfer modelling suggest that this upper flux limit corresponds to an upper limit to the abundance of wide spread water vapour, $X(H_2O) < 10^{-6}$ to 10^{-5}, in the ρ Oph cloud.
- Comparison of $X(H_2O)$ with the evolutionary molecular cloud models, including shock chemistry due to outflows from young stellar objects, by Bergin et al. (1998) leads to an estimate of the time the ρ Oph cloud has been forming stars, viz. for less than 10^6 years ($2 - 5 \times 10^5$ yr).

Acknowledgements. We thank David Neufeld for valuable suggestions in his referee report. Alexis Brandeker is thanked for his assistance with the *c*-programming. This work was supported by the Swedish National Space Board.

References

André P., Ward-Thompson D., Barsony M., 1993, ApJ 406, 122
Bergin E.A., Melnick G.J., Neufeld D.A., 1998, ApJ 499, 777 (BMN)
Bontemps S., Nordh L., Olofsson G., et al., 1999, to be submitted to A&A
Chandra S., Varshalovich D.A., Kegel W.H., 1984, A&AS 55, 51
Clegg P.E., Ade P.A.R., Armand C., et al. 1996, A&A 315, L 38
Gómez M., Whitney B.A., Wood K., 1998, AJ 115, 2018
Greene T.P., Meyer M.R., 1995, ApJ 450, 233
Harstein D., Liseau R., 1998, A&A 332, 703
Kessler M.F., Steinz J.A., Anderegg M.E., et al., 1996, A&A 315, L 27
Lada C.J., 1985, ARA&A 23, 267
Liseau R., Lorenzetti D., Molinari S., et al., 1995, A&A 300, 493
Liseau R., White G.J., Larsson B., et al., 1999, A&A 342, in press
Melnick G.J., Dalgarno A., Erickson N.R., et al., 1997, ESA SP-401, p. 189
Nordh H.L., 1997, ESA SP-401, p. 195
Phillips T.R., Maluendes S., Green S., 1996, ApJS 107, 467
Sekimoto Y., Tatematsu K., Umemoto T., et al., 1997, ApJ 489, L 63
Shu F.H., Adams F.C., Lizano S., 1987, ARA&A 25, 23
Staude H.J., Elsässer H., 1993, A&AR 5, 165
Swinyard B.M., Clegg P.E., Ade P.A.R., et al., 1996, A&A 315, L 43
Tamura M., Sato S., Kaifu N., et al., 1990, ApJ 350, 728
Wilking B.A., Lada C.J., 1983, ApJ 274, 698
Wilking B.A., Schwartz R.D., Fanetti T.M., Friel E.D., 1997, PASP 109, 549